Dramatic Photoinduction of Hole Tunneling in Double Quantum Wells with Built-In Piezoelectric Fields

Philippe Boring and Bernard Gil
Groupe d'Etudes des Semiconducteurs, Université de Montpellier II, Case Courrier 074, 34095 Montpellier Cedex 5, France

Karen J. Moore
Department of Mathematics and Physics, The Manchester Metropolitan University, John Dalton Building, Chester Street, Manchester M1 5GD, United Kingdom
(Received 2 June 1993)

We show that efficient tunneling of holes can be produced in double quantum wells with built-in piezoelectric fields by the photoscreening of that piezoelectric field. Our observation was made at low temperatures by comparing the behavior of $Ga_{0.92}In_{0.08}As$-GaAs strained-layer double quantum wells grown along the (111) and (001) directions and tuning the densities of photoinjected carriers over several decades. Interpretation of the experimental data is made by comparison with Hartree calculations including the space charge effects. In addition to this, we also report the observation of many-body interactions at high photocarrier densities.

PACS numbers: 73.20.Dx, 71.55.Eq, 73.40.Gk, 78.55.Cr

When P. and J. Curie discovered piezoelectricity in 1880, they probably did not imagine the full impact this universal property of crystals without inversion symmetry could have on every day life. This coupling between electrical and mechanical properties leads to numerous applications. The acuity of the mechanical resonance of piezoelectric devices has repercussions on the electrical properties and has long since been used in electronics for signal filtering (using surface acoustic waves) or making surface-acoustic memories. More recently, Smith and Mailhiot [1] suggested that advantage be taken of such an effect to produce significant nonlinear optical behavior in some strained-layer semiconductor quantum wells and superlattices. Experimental confirmation of their predictions has now appeared in the literature [2–9]. We also recently reported the observation of dramatic band gap renormalization under photoillumination [10].

In this Letter, we show that double quantum wells may exhibit very interesting properties when carrier tunneling can be easily photocontrolled. We have studied photoinduced tunneling in the (Ga,In)As-GaAs system, which due to the combined effects of the potential depths, and the values of the Luttinger parameters γ_1 and γ_3, is an ideal system to investigate hole rather than electron tunneling.

The layers were all deposited by molecular beam epitaxy in a Varian modular Gen II growth system. The samples were deposited simultaneously on undoped, (001) GaAs substrates and n^+ ($\sim 2\times 10^{18}$ cm^{-3}), (111)*B*-oriented GaAs substrates. The (001) and (111)*B* substrates were indium bonded side by side to an indium free mounted GaAs substrate. The substrate temperature during growth was nominally 520 °C. Growth rates for both the GaAs and (InGa)As were measured using the RHEED oscillation technique on a GaAs monitor slice prior to growth of the quantum well samples. For the purpose of these investigations two types of structures were studied. In both cases the growth sequence commenced with the deposition of a 0.5 μm undoped GaAs layer. We note that thick, nominally undoped layers grown in this apparatus have a low ($\sim 10^{15}$ cm^{-3}) *p*-type residual impurity concentration. This is followed by a double quantum well structure consisting of two 4.9 nm $Ga_{0.92}In_{0.08}As$ layers separated by a 2.2 nm thin unintentionally doped GaAs barrier layer. The quantum well and barrier layers are undoped. Both structures are completed by a second 0.5 μm undoped GaAs layer and finally a 2 μm beryllium-doped ($p^+ \sim 2\times 10^{18}$ cm^{-3}) GaAs layer. The Fermi level is pinned to the top of the valence/conduction band in the p^+/n^+ regions, respectively, giving a 1.5×10^4 V/cm *nip* field in the undoped region of the samples. Moreover, (111) substrates were chosen to be (111)*B* oriented so that the piezoelectric field which equals some 1.25×10^5 V/cm in the strained layers is opposite to the *nip* field [11]. Figure 1 illustrates the differences between the band lineups and first conduction and heavy hole valence band envelope functions for the two kinds of samples. Low temperature (4 K) photoluminescence measurements were made with the samples mounted on the cold finger of a variable temperature, continuous flow cryostat. The excitation source was an Ar^+ pumped Ti-sapphire laser tuned to 810 nm. The excitation density was varied by changing the laser power over more than 3 orders of magnitude while taking care to ensure that the sample was not heated.

The evolution of the photoluminescence spectra with pump power is shown in Fig. 2(a), for the (111)*B* sample. We note the evolution of an additional line near 1458 meV, at some 10 meV above the fundamental line, as the excitation density is increased. In addition, we detect emission below the signature of the main photoluminescence due to donor-acceptor pairs in the substrate. The identification of these lines is made by comparison with the numerical calculation described below. Focusing on

0031-9007/93/71(12)/1875(4)$06.00

the e_1hh_1 transition, it is clear that the magnitude of the observed blueshift cannot only be related to a screening of the excitonic interaction (a couple of meV in this sample) by the plasma, but that additional effects occur. A control experiment was done for the identical (001) double quantum well for which the piezoelectric effect does not exist and the results are shown in Fig. 2(b). None of the dramatic effects characteristic of the (111) structure was observed.

To explain our observations we must consider a number of phenomena. First, the effect of space charge fields caused by the spatial separation of photoinjected electron and holes. Referring to Fig. 1, it is obvious that this is more efficient for the $(111)B$ sample than for the (001) one. This is confirmed by theory and we will limit this Letter to the $(111)B$ sample for which the effects are dramatic.

To quantify the space effect, and in the simplest approach, we have to solve self-consistently the equation

$$\left[-\frac{\hbar^2}{2}\frac{\partial}{\partial z}\left(\frac{1}{m_i^*(z)}\right)\frac{\partial}{\partial z}+V(z)+q[F(z)+\Phi(z)]z\right]\chi(z)=E\chi(z) \tag{1}$$

for each type of carrier. In this equation, V is the potential lineup, F is the total field without injected carriers, and Φ is the contribution of photoinjected electron-hole pairs. At low temperatures we approximate the Fermi distribution by a step function and define Φ as follows:

$$\Phi(z+dz)-\Phi(z)=e\sigma\int_z^{z+dz}\left[\sum_{m,i}\int_0^{k_\perp(\sigma)}a_{m,i}(k_\perp,\sigma)\chi^2_{h_{m,i}}(k_\perp,u)dk_\perp-\sum_{n,j}\int_0^{k_\perp(\sigma)}\beta_{n,j}(k_\perp,\sigma)\chi^2_{e_{n,j}}(k_\perp,u)dk_\perp\right]\frac{du}{\epsilon(u)},$$

where the summations are extended over the n electron (e) and m hole (h) states for a given areal carrier density σ, by the phase space filling which occurs up to an appropriate value of the in plane wave vector $k_\perp$. The indices i and j refer to the lifting of spin degeneracy away from $k_\perp=0$, and $\epsilon(z)$ is the dielectric constant.

Figure 3 shows self-consistent calculations of the energy differences between different hole states and the first heavy hole state. A similar plot is also given for the electrons. For the sake of completeness, we report the evolution of the filling energy E_f of the fundamental subbands in relationship with a Fermi vector $k_f=(2\pi\sigma)^{1/2}$ via a parabolic model for both conduction and valence states. As σ (laser intensity) is increased, the different hole states tunnel through the structure; the most dramatic tunneling occurs for hh_2 near $\sigma\sim6\times10^{11}$ cm^{-2}. For values of σ beyond the critical value $\sigma_c\sim5.5\times10^{11}$ cm^{-2} at which the crossing of $E_f(hh_1)$ with curve hh_2-hh_1 occurs, population of several subbands has to be included in the calculation. We also note that two electron bands are filled at $\sigma\sim7\times10^{11}$ cm^{-2}.

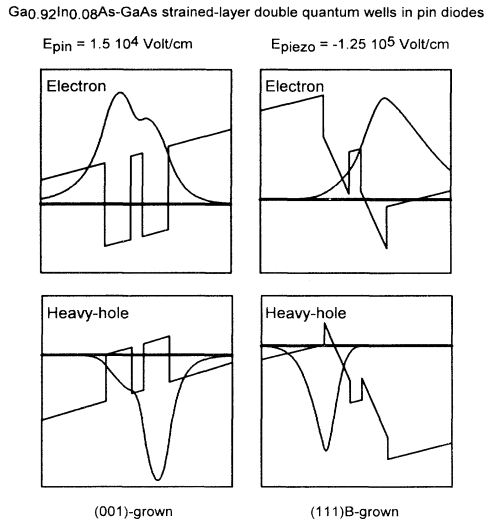

FIG. 1. Schematic of the potential lineups, wave functions, and confined levels which illustrate the difference between (001)- and (111)-oriented GaInAs-GaAs double quantum wells at $\sigma=0$.

The resulting wave functions are given in Fig. 4 for two plasma densities. To simplify the figure, we limit the plot to the first conduction state and the two lowest heavy hole levels. The alteration of the potential lineups provoked by the photoinjected plasma is inserted in the figure as well as the position of the self-consistent energies.

To summarize the different aspects of the calculation and in order to interpret the experimental data we have plotted the characteristic transition energies of this double quantum well as a function of the areal carrier densities in Fig. 5(a). The area of the circles is proportional to the square of the overlap integral between the electron and hole envelope functions. The photostimulation of the hole tunneling is clearly apparent in Fig. 5(b) where the average position of the particles in different quantum states is plotted [the origin corresponds to the left-hand GaAs-(InGa)As interface]. The sudden tunneling of the second heavy hole is connected to the change of the overlap integral e_1hh_2 illustrated in Fig. 5(c) and to the simultaneous decrease of the hh_2-hh_1 splitting.

Returning to the experimental data reported in Fig. 2(a), we are now able to identify all the photoluminescence lines. The onset of photoluminescence at 1458 meV (e_1hh_2), for a pump density of 215 W/cm^{-2} is interpreted in terms of filling the hh_2 band. This corresponds to $\sigma_c=5.5\times10^{11}$ cm^{-2} in our calculation. The weakness of this peak is interpreted in terms of a weak thermal population ($T=4$ K, not 0 K) of the second heavy hole subband. We estimate that this phenomenon

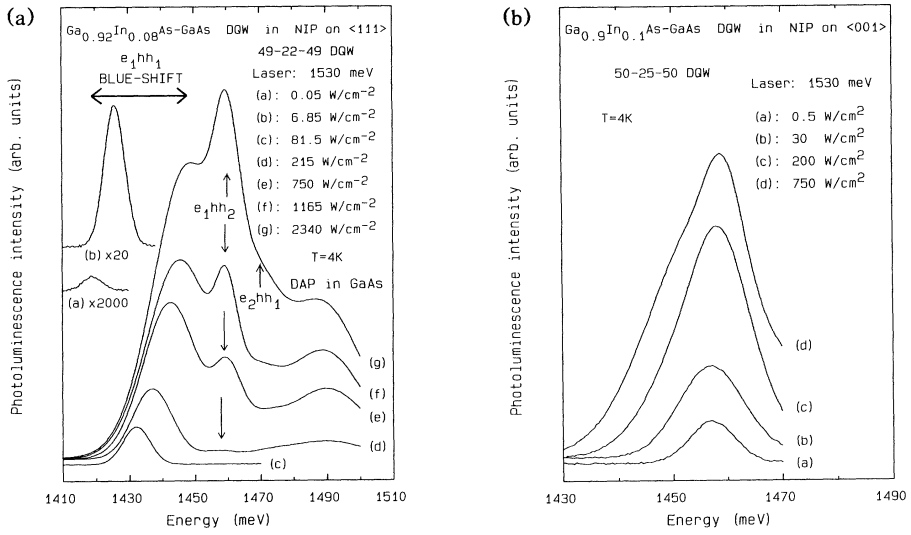

FIG. 2. (a) Pump power dependence of the photoluminescence of the (Ga,In)As-GaAs strained-layer double quantum well (111)*B* grown. Note the dramatic blueshift of the fundamental line and the occurrence of additional features as the intensity increases. (b) Analog of (a) but for the (001) sample.

occurs at $\sigma = 5\times10^{11}$ cm^{-2}. Focusing on the experimental value of the e_1hh_2-e_1hh_1 splitting (12 meV), we note that the calculated value at saturation ($\sigma_s \sim 10^{12}$ cm^{-2}) is 3 meV. This reflects the nonlinear relationship between the laser power and the active areal density of photocarriers. Beyond $\sigma = 7\times10^{11}$ cm^{-2}, as stated above, the second electron band is filled. Increasing the areal density of active *e-h* pairs then becomes almost impossible, due to the existence of the *pin* field which causes an efficient tunneling of the e_2 electron away from the double quantum well. This leads to an equilibrium limit where recombination processes are no longer dominated by photogeneration. The 1470 meV photoluminescence feature can thus be attributed to e_2hh_1.

Another important effect can occur at these plasma densities: the onset of band gap renormalization produced by the many-body interaction in the plasma [10, 12–21]. Model calculations of this effect have shown that it can be given roughly by a positive power law of the carrier density. We expect excellent agreement between the one particle calculation and the experiment at very low densities, but this agreement should diminish at high photoinjection when the physics is dominated by many-body effects [10]. This is in accord with the significant discrepancy between our high density data and the Hartree calculation. At $\sigma_s = 10^{12}$ cm^{-2}, we estimate the band gap renormalization to be some 26 meV for e_1hh_1 and 17 meV for e_1hh_2 while the renormalization at $\sigma = 5\times10^{11}$ cm^{-2} is approximately 25 and 8 meV, respectively. We interpret the almost identical band gap renormalization of e_1hh_1 at these two concentrations on the basis of arguments linked to the distribution of elec-

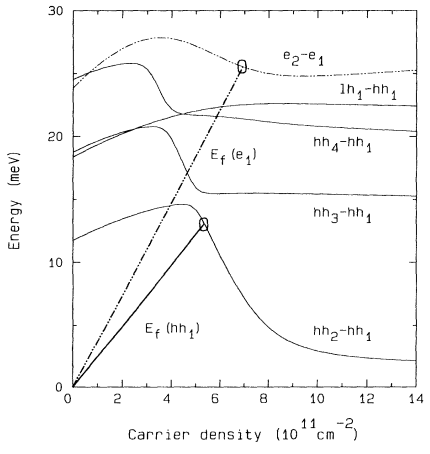

FIG. 3. Energy separation between valence and conduction subbands as a function of the areal carrier density, for the (111)*B* sample. The Fermi energies are also plotted.

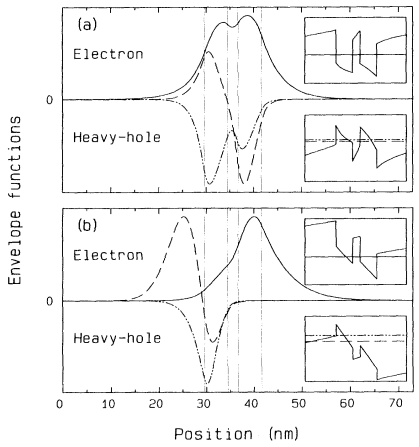

FIG. 4. Plot of self-consistent wave functions for the first electron and two heavy hole confined states, for the (111)*B* sample. The potential lineups and positions of the confined states are inserted. The data are given for two areal carrier concentrations [carrier density (10^{11} cm^{-2})]: (a) 14; (b) 1.

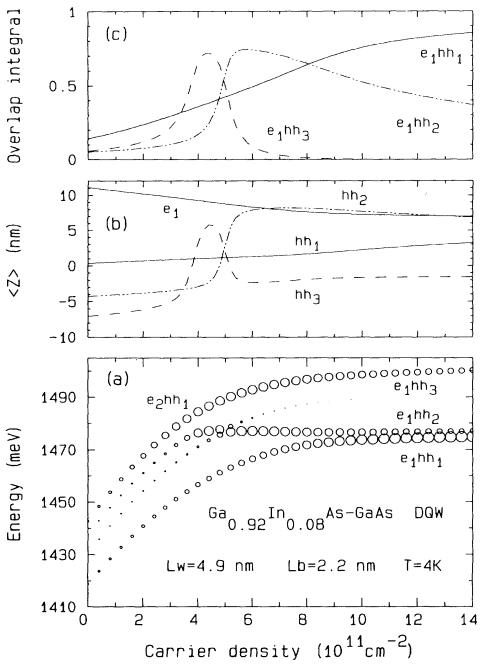

FIG. 5. Plot of typical data obtained from the self-consistent calculation including (a) transition energies, (b) average particle positions, and (c) overlap integral for the sample with piezoelectric field. See text for details.

trons and holes in the various states [20,21]. At $\sigma_s = 10^{12}$ cm^{-2} the heavy hole is shared almost identically between the two lowest subbands, while at $\sigma = 5\times10^{11}$ cm^{-2}, the population occurs only in the first heavy hole subband. Moreover, when $\sigma > 7\times10^{11}$ cm^{-2}, electrons start to fill the second electronic subband e_2. Thus, at σ_s, the population of the fundamental electronic subband is $< 10^{12}$ cm^{-2} (8.5×10^{11} cm^{-2} in the parabolic model). Considering e_1hh_2, the weak renormalization at $\sigma = 5\times10^{11}$ cm^{-2} (8 meV) can be explained in terms of a vanishingly small population of the hh_2 subband. When σ is increased to $\sigma_s = 10^{12}$ cm^{-2}, there is a significant hh_2 population producing some 17 meV band gap renormalization.

In conclusion, we have shown that photoinduced tunneling of holes can be produced in double quantum wells with internal built-in piezoelectric fields. This is based on the screening of the piezoelectric field by the photo plasma which also produces significant band gap renormalization.

[1] The essential aspects of their contribution to the field can be found in D. L. Smith and C. Mailhiot, Rev. Mod. Phys. **62**, 173 (1990); and in C. Mailhiot and D. L. Smith, Crit. Rev. Solid State Mat. Sci. **16**, 131 (1990).

[2] B. Laurich, K. Elcess, C. G. Fonstad, J. G. Beery, C. Mailhiot, and D. L. Smith, Phys. Rev. Lett. **62**, 649 (1989).

[3] E. A. Caridi, T. Y. Chang, K. W. Goosen, and L. F. Eastman, Appl. Phys. Lett. **56**, 659 (1990); K. W. Goosen, E. A. Caridi, T. Y. Chang, J. B. Stark, D. A. B. Miller, and R. A. Morgan, Appl. Phys. Lett. **56**, 715 (1990).

[4] B. K. Laurich, D. L. Smith, D. E. Watkins, I. Sela, S. Subanna, and H. Kroemer, Superlattices Microstruct. **9**, 499 (1991); I. Sela, D. E. Watkins, B. K. Laurich, D. L. Smith, S. Subanna, and H. Kroemer, Appl. Phys. Lett. **58**, 684 (1991).

[5] B. V. Shanabrook, D. Gammon, R. Beresford, W. I. Wang, R. P. Leavitt, and D. A. Broido, Superlattices Microstruct. **7**, 363 (1990); G. Brozak, B. V. Shanabrook, D. Gammon, D. A. Broido, R. Beresford, and W. I. Wang, Surf. Sci. **267**, 120 (1992).

[6] R. André, C. Deshayes, J. Cibert, Le Si Dang, S. Tatarenko, and K. Saminadayar, Phys. Rev. B **42**, 11392 (1990); J. Cibert, R. André, C. Deshayes, Le Si Dang, H. Okumura, S. Tatarenko, G. Feuillet, P. H. Jouneau, R. Mallard, and K. Saminadayar, J. Cryst. Growth **117**, 424 (1992).

[7] M. P. Halsall, J. E. Nicholls, J. J. Davies, B. Cockayne, and P. J. Wright, J. Appl. Phys. **71**, 907 (1992).

[8] T. S. Moise, L. J. Guido, J. C. Beggy, T. J. Cunningham, S. Seshadri, and R. C. Barker, J. Electron. Mater. **21**, 119 (1992); T. S. Moise, L. J. Guido, R. C. Barker, J. O. White, and A. R. Kost, Appl. Phys. Lett. **60**, 2637 (1992).

[9] M. Lakrimi, R. W. Martin, C. Lopez, D. M. Symons, E. T. R. Chidley, R. J. Nicholas, N. J. Mason, and P. J. Walker, Semicond. Sci. Technol. **8**, 367 (1993).

[10] K. J. Moore, P. Boring, B. Gil, and K. Woodbridge (unpublished).

[11] D. L. Smith, Solid State Commun. **57**, 919 (1986).

[12] G. E. W. Bauer and T. Ando, Phys. Rev. B **31**, 8321 (1985); J. Phys. C **19**, 1537 (1986); Phys. Rev. B **34**, 1300 (1986).

[13] D. A. Kleiman and R. C. Miller, Phys. Rev. B **32**, 2266 (1985); D. A. Kleiman, Phys. Rev. B **33**, 2540 (1986).

[14] S. Schmitt-Rink, D. S. Chemla, and D. A. B. Miller, Phys. Rev. B **32**, 6601 (1985); S. Schmitt-Rink, C. Hell, and H. Haug, Phys. Rev. B **33**, 1183 (1986); A. E. Ruckenstein and S. Schmitt-Rink, Phys. Rev. B **35**, 7551 (1987).

[15] G. Bongiovanni and J. L. Staehli, Phys. Rev. B **39**, 8359 (1989); **46**, 9861 (1992).

[16] S. das Sarma, R. Jalabert, and S. R. Eric-Yang, Phys. Rev. B **41**, 8288 (1990).

[17] R. Binder, I. Galbraith, and S. W. Koch, Phys. Rev. B **44**, 3301 (1991).

[18] P. Von Allmen, Phys. Rev. B **46**, 13345 (1992).

[19] C. Delalande, G. Bastard, J. Orgonasi, J. A. Brum, H. W. Liu, M. Voos, G. Weimann, and W. Schlapp, Phys. Rev. Lett. **59**, 2690 (1987).

[20] C. Weber, C. Klingshirn, D. S. Chemla, D. A. B. Miller, J. E. Cunningham, and C. Hell, Phys. Rev. B **38**, 12749 (1987).

[21] J. C. Ryan and T. L. Reinecke, Phys. Rev. B **47**, 9615 (1993).